

Compressible Unsteady Aerodynamic Loads on Oscillating Airfoils in a Subsonic Flow

Ahmed I. El-Nadi*, Nabil M. Khalifa[†] and Haithem E. Taha[‡] *University of California, Irvine, CA, 92697, USA*

The compressible aerodynamic loads on a plunging flat plate are computed using Mathieu functions for different subsonic Mach numbers and a large range of reduced frequency (0-15). The obtained results are validated using previous theoretical ones and unsteady inviscid computational fluid simulations. Results show that the normalized circulatory lift magnitude decreases as frequency increases. The non-circulatory lift reaches an asymptotic value with increasing frequencies, in contrast to the behavior of the incompressible fluid. Also, a considerable phase shift in the lift response is found for small reduced frequencies, which diminishes at high oscillation frequency. Finally, it is found that compressibility has an insignificant effect on the aerodynamic loads at low frequencies.

I. Nomenclature

a =Semi-Chord Length.

c = Speed of sound in undisturbed flow.

C = Flat plate chord

 $C(\mu)$ = Circulatory lift frequency response.

 ce_m , se_m = Cosine elliptic and sine elliptic angular Mathieu functions, respectively, of order m.

H = Plunging amplitude. K = Radian Frequency. L_c = Circulatory Lift. L_{nc} = Non-Circulatory Lift.

 $Mc_i^{(j)}$, $Ms_i^{(j)}$ = Radial Mathieu functions of kind j and order i

u = Velocity disturbance in X-direction.
 φ = Perturbation velocity potential.
 v = Vertical velocity magnitude.

 p, ρ = Perturbation pressure and density, respectively.

 $\Phi = \text{Total velocity potential.}$ $\Phi_o = \text{Steady velocity potential.}$ $\phi = \text{Transient velocity potential.}$ $\rho_o = \text{Undisturbed fluid density.}$ $\mu = \text{Reduced Frequency.}$

v = Compressible Reduced Frequency.

II. Introduction

Computation of the aerodynamic loads over an airfoil in steady incompressible flow has been an active topic of cresearch over the last century. However, in actual flight conditions, the aeroelastic stability formed a challenge that researchers need to overcome by accounting for unsteadiness. Despite being vital in the development of aviation, the unsteady aerodynamic theories should be extended to account for compressibility and viscosity effects. The unsteady theories are complex by nature; therefore, Lin [1] and Miles [2] established the linearization of the governing equation. They discussed the linearization limits based on the lifting surface motion amplitude, Mach

^{*}Msc student, Mechanical and Aerospace Engineering, 5200 Engineering Service Rd, Irvine, CA 92617, AIAA student member

[†]Phd student, Mechanical and Aerospace Engineering, 5200 Engineering Service Rd, Irvine, CA 92617, AIAA student member

^{*}Associate Professor, Mechanical and Aerospace Engineering, 5200 Engineering Service Rd, Irvine, CA 92617, AIAA Senior member.

number, and frequency. This research effort was launched by Theodorsen [3] publication on flutter characteristics in a two-dimensional incompressible flow. Theodorsen decomposed the total lift force into "circulatory" and "non-circulatory" components. As a side, this classification is ambiguous [4] as both components have interacting effects.

Extending the unsteady theories to account for compressibility is not straightforward as the flow is no longer governed by the Laplace equation, rather by the wave equation. Moreover, the pressure waved travel to infinity at a speed equal to the speed of sound. Possio [5] calculated the aerodynamic coefficients of oscillating airfoils in a subsonic compressible flow, replacing the airfoil with a doublet distribution in the form of an integral equation known as Possio's integral equation. He obtained an approximate solution of the integral equation by expressing the doublet intensity in a series form. Attempts to obtain an accurate solution of possio's integral equation continued by Schade [6] and Dietze [7]. Schade approximated the integral equation in a set of algebraic equations and Dietze solved the equation iteratively. Later, Miles [8] expanded the kernel function of the integral equation in powers of Mach number. A different integral equation solution of the wave equation is derived from green's function of the first kind by W.P. Jones [9],[10]. He provided an approximate solution to the integral equation at the boundary and calculated the aerodynamic coefficients for pitching and plunging airfoil. His results showed a good agreement to the exact solution by I.T. Minhinnck [11].

Separation of variables had alternatively been used to solve the compressible flow problem. For this solution, the flow field is expressed in either the velocity or acceleration potential with related methods known, in literature, as "method of velocity potential" and "method of acceleration potential", respectively. Haskind [12], Ressiner [13], R. Timman [14], R. Timman and Adriaan Isak [15] and Mazelsky [16] used the method of velocity potential and found a solution in terms of Mathieu functions. They separated the total velocity potential into a regular (non-circulatory) solution, satisfying the no penetration boundary condition and a singular (circulatory) solution that has a zero normal derivative at the trailing edge. Mazelsky derived the aerodynamic coefficients formulas for a vanishing aspect ratio airfoil and tabulated the lift and rolling moment coefficients for compressible and incompressible flow for a wide range of reduced frequencies. His results showed a negligible effect of compressibility for small values of reduced frequencies. However, for higher reduced frequencies, the compressibility effects are robust.

The acceleration potential method was adopted by Hofsommer [17], Kussner [18] and Timman and Van De Vooren [19]. The regular solution is similar to the velocity potential solution. For the singular solution, the Laplace equation is replaced by a solution of the wave equation that adds correction terms for compressible flow and satisfies zero normal velocity derivative on the surface. Timman and Van de Vooren [20] obtained results for aerodynamic coefficients of an oscillating airfoil in compressible flow at five values of Mach numbers and frequencies ranging from 0.1 to 3. Their results diverged from Dietze's [21] solution of Possio's integral equation.

In this article, we provide numerical computations for circulatory lift and non-circulatory lift for compressible flow over a flat plate based on Haskind's[12] method at three values of Mach numbers (M=0.35, 0.5 and 0.6). Computations are performed using MATLAB code for solving Mathieu equations. Code accuracy and reduced frequency effects on the error produced in Mathieu function computations were investigated. The results are validated against previous theoretical results and unsteady inviscid Computational Fluid Dynamic (CFD) simulations were performed to examine the validity of the theory at high frequencies.

The present article comprises seven sections. Section III of this article summarizes Haskind's [12] derivation with minor corrections. The circulatory and non-circulatory lift frequency response analytical results are presented in section IV. The CFD setup is illustrated with mesh properties in section V. In section VI, the lift results for plunging motion are presented and compared with simulations.

III. Theoretical Background

This section presents a summary of Haskind's [12] derivation, including the governing equations, boundary, and initial conditions for plunging motion. Some formulas mentioned in this section are in a simplified form of the original derivation. Moreover, the symbols are identical to the original counterpart except for Mathieu functions as we adopted Abramowitz [22] notations.

A. Governing Equations and Boundary Conditions

A plan two-dimensional wing of infinite span performing a sinusoidal plunging motion is placed in a compressible fluid with a mean velocity component U in positive X-direction. The linearized perturbation velocity potential equation has the form,

$$(1 - M^2)\frac{\partial^2 \Phi}{\partial X^2} + \frac{\partial^2 \Phi}{\partial Y^2} + 2\frac{M}{c}\frac{\partial^2 \Phi}{\partial X \partial t} - \frac{1}{c^2}\frac{\partial^2 \Phi}{\partial t^2} = 0$$
 (1)

where $c=\sqrt{\gamma dp/d\rho}$. The total velocity potential is divided into a steady-state component, Φ_o , and a transient component, φ , corresponds to the oscillatory motion. The steady state solution is simple and out of scope of our present study. The non-dimensional coordinates $x=\frac{X}{a}$ and $y=\sqrt{1-M^2}\frac{Y}{a}$ are introduced. The reduced frequency, $\mu=\frac{Ka}{U}$, and Mach number, $M=\frac{U}{c}$, are famous resulting non-dimensional variables.

The vertical oscillation velocity is defined as $V(x) = v \ e^{(iKt)}$, where v is the vertical velocity amplitude. Substituting the non-dimensional variables and plunging motion defined above into Eq. (1). The resulting governing equation and boundary conditions will be expressed as:

$$\frac{\partial^2 \varphi}{\partial x^2} + \frac{\partial^2 \varphi}{\partial y^2} + v^2 \varphi = 0, \tag{2}$$

$$|X| \le 1, \quad y = 0, \qquad \frac{\partial \varphi}{\partial y} = \frac{a}{\sqrt{1 - M^2}} e^{(i\lambda x)} = V(x),$$
 (3)

$$X > 1, \quad y = 0, \qquad \varphi = 0, \tag{4}$$

$$X < -1, \quad y = 0, \qquad \frac{\partial \varphi}{\partial x} - i\alpha \varphi = 0,$$
 (5)

where $v = \frac{\mu M}{1 - M^2}$, $\lambda = \frac{M^2 \mu}{1 - M^2}$ and $\alpha = \frac{\lambda}{M^2}$. Equation. (2) and its corresponding boundary conditions are the famous exterior boundary value problem. A solution in the form of Mathieu equations is obtained by transforming Eqns. (2)-(5) into elliptic coordinates, which have the form:

$$\varphi(\zeta,\eta) = \varphi_o + \psi = \sum_{n=0}^{\infty} b_n c e_n(\zeta) M c_n^{(4)}(\eta) + \sum_{n=0}^{\infty} a_n s e_n(\zeta) M s_n^{(4)}(\eta). \tag{6}$$

For more details about Mathieu functions code validation and computational accuracy, reader is referred to appendix A.

B. Non-Circulatory Lift

From Eqn. (6) the non-circulatory component is given by

$$\varphi_o = \sum_{n=0}^{\infty} a_n s e_n(\zeta) M s_n^{(4)}(\eta). \tag{7}$$

The non-circulatory pressure distribution over the airfoil surface is obtained by substituting the no-penetration boundary condition into Eq. (7) and have the form

$$p = \frac{\rho_o U}{a} e^{i(kt - \lambda \cos \eta)} \left[-\frac{1}{\sin \eta} \sum_{n=1}^{\infty} a_n s e'_n(\eta) M s_n^{(4)}(0) - i\alpha \sum_{n=1}^{\infty} a_n M s_n^{(4)}(0) s e_n(\eta) \right]. \tag{8}$$

From Eqn. (7), the non-circulatory lift over the airfoil surface is

$$L_{nc} = 2\rho_{o}U \sum_{n=1}^{\infty} a_{n} M s_{n}^{(4)}(0) e^{ikt} \int_{0}^{\pi} e^{-i\lambda \cos \eta} \left[-i\alpha \sin \eta \ s e_{n}(\eta) - s e_{n}^{'}(\eta) \right] d\eta, \tag{9}$$

where the value of coefficient a_n depends on the type of motion.

C. Circulatory Lift

From Eqn. (7), the circulatory component of the velocity potential will be

$$\psi = \sum_{n=0}^{\infty} b_n c e_n(\zeta) M c_n^{(4)}(\eta). \tag{10}$$

Introducing function W(x, y), related to the function ψ as

$$\frac{\partial \psi}{\partial x} - i\alpha\psi = \frac{\partial w}{\partial y},\tag{11}$$

Satisfying the differential equation $\nabla^2 w + v^2 w = 0$ and the radiation condition at infinity. Applying the boundary condition over the surface of the airfoil, $|x| \le 1$, a solution of the function W(x, y) is obtained as $w(x, 0) = Ae^{ivx} + Be^{-ivx}$ for y = 0, $|x| \le 1$. Haskind [12], also, expressed w(x, z) in an integral form by excluding the sources on the airfoil (-1, +1) as

$$w(x,y) = \int_{-1}^{+1} \gamma(s) H_0^{(2)}(vr) ds, \qquad r^2 = (x-s)^2 + y^2, \tag{12}$$

where $\gamma(s)$ is expressed as summation of angular and radial Mathieu functions. Equation (12) satisfies boundary conditions and radiation principle at infinity. Two equations relating the coefficients A and B are required to solve the circulatory lift problem. With the aid of Eq. (12) and satisfying the boundary conditions on the plane of symmetry and the radiation condition at infinity, an equation relating constants A and B have the form

$$A\left(C_{+} + \frac{i e^{i(\nu - \alpha)}}{\nu - \alpha}\right) + B\left(C_{-} - \frac{i e^{-i(\nu + \alpha)}}{\nu + \alpha}\right) = 0 *$$

$$\tag{13}$$

where

$$c_{\pm} = \frac{1}{2i} \sum_{m=0}^{\infty} M c_m^{(4)'}(0) \ \alpha_{\pm}^{(m)} \int_0^{\pi} f(\cos \zeta) \ c e_m(\zeta) \ d\zeta, \qquad \alpha_{\pm} = \frac{\int_0^{\pi} e^{\pm i \nu \cos \zeta} c e_m(\zeta) d\zeta}{M c_m^{(4)}(0) \int_0^{\pi} \left[c e_m(\zeta) d\zeta \right]}^{\dagger}$$
 (14)

$$f(\cos\zeta) = e^{-i\alpha\cos\zeta} \int_{\infty}^{1-\cos\zeta} e^{-i\alpha\xi} H_0^{(2)}(v\xi) d\xi^{\ddagger}$$
 (15)

A second equation relating A and B is obtained by satisfying trailing edge finite velocity (Kutta condition). The circulatory Lift amplitude is obtained in away similar to the non-circulatory lift.

IV. Compressible Circulatory and Non-circulatory Lift Frequency Response

Plunging circulatory and non-circulatory lift frequency responses are presented in this section for a range of reduced frequencies of 0 to 15 and multiple values of Mach numbers using normalized plunging magnitude $\frac{\overline{H}}{C} = 0.001$. The circulatory lift frequency response, $C(\mu)$, is the ratio of the circulatory lift, L_c , to the quasi-steady lift, $L_{QS} = 2\pi i \rho_o U^2 a \mu \overline{H} e^{iKt}$. Figures 3a and 3b show the circulatory lift frequency response magnitude and phase, respectively. As shown in the figures, the function magnitude decreases as the Mach number increases. The high frequency gain of the frequency response approaches zero asymptotically. Also, there exists a significant phase lag between the plate motion and resulting lift; the lag is almost independent of the reduced frequency.

Similar to the circulatory frequency response, the non-circulatory frequency response is the ratio of the non-circulatory lift, L_{nc} , to the quasi-steady lift. For a plate oscillating in an incompressible fluid, the non-circulatory frequency response increases as the reduced frequency increases and responds promptly with a 90° phase difference. However, in the case of a compressible fluid, the non-circulatory frequency response tends to be independent of the reduced frequency for high frequency values, as shown in figure 2a. Moreover, the function magnitude decreases as the Mach number increases. Finally, from figure 2b, the phase difference decreases with frequency and converges to zero asymptotically.

^{*} A minus sign is missing in the exponential in the second bracket in Haskind[12] formulation.

[†] This expression is reformulated to cancel normalization.

[‡] Analytical solution of the infinite integral in the Appendix B.

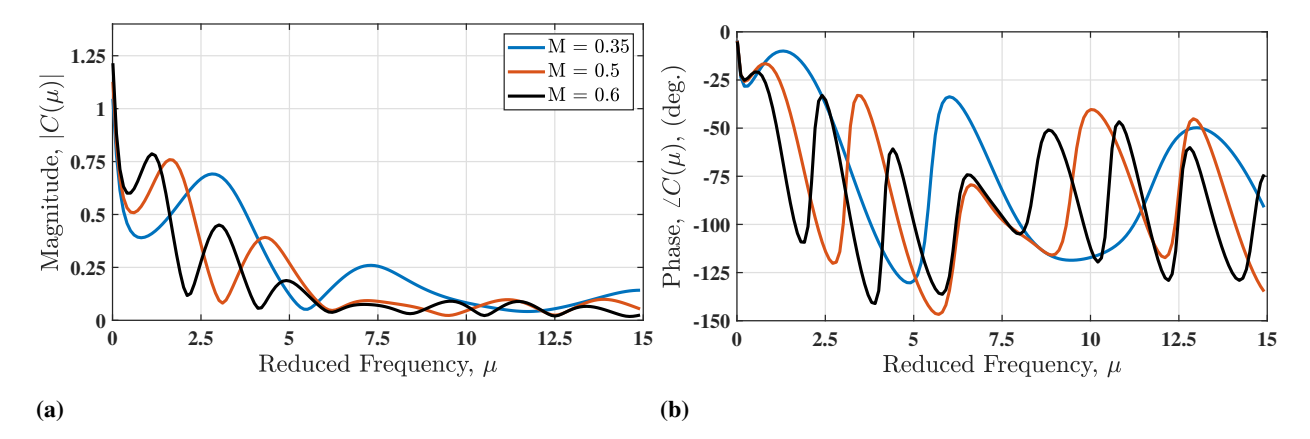


Fig. 1 Analytical results of plunging circulatory lift frequency response at different compressible Mach numbers. (a) Circulatory lift frequency response magnitude vs. reduced frequency. (b) Phase vs reduced frequency.

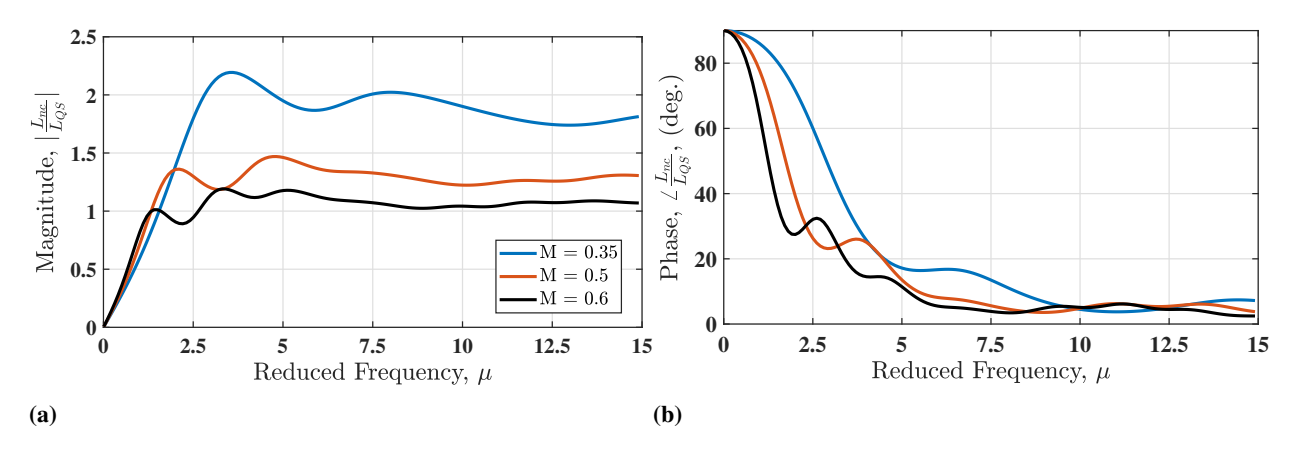


Fig. 2 Analytical results of plunging non-circulatory lift frequency response at different compressible Mach numbers. (a) Non-circulatory lift magnitude vs. reduced frequency. (b) Non-circulatory lift phase vs. reduced frequency.

V. Computational Simulation

Simulations using Navier-Stokes equations were performed to validate the theoretical results and examine the theory robustness at high frequencies. The simulations were proceeded using ANSYS FLUENT 20.1 package. The plunging motion is defined using velocity oscillation as

$$V(t) = v\cos\left(Kt\right) \tag{16}$$

where $v = \overline{H} \times K$, guarantying the validity of small perturbation analysis. The flat plate has a half chord length of 0.5 m.

A. Computational Grid

A two-dimensional structured O-grid is generated using ICEM CFD package. For grid quality purposes, the flat plate assumption was replaced by a rectangle of length 1 m and a thickness of $10^{-4}m$. As shown in Figure (3), the computational grid is divided into three rings. The inner ring is 5c in radius. This region has a dense mesh to capture the shed vertices from the trailing edge. The first cell, on the flat plate surface, height is $1 \times 10^{-6} c$ with an expansion ration of 1.1. A total number of 160 cells is used on each side of the flat plate. To maintain a high-quality mesh near the flat plate surface, the inner ring and the flat plate move as a rigid body performing the plunging motion using a user defined function (UDF). The intermediate ring has an outer radius of 9 c. The dynamic mesh motion is assigned to the intermediate ring with a deforming technique to absorb the inner ring motion. The outer ring has an outer radius of 12.5 c0 with stationary outer boundary.

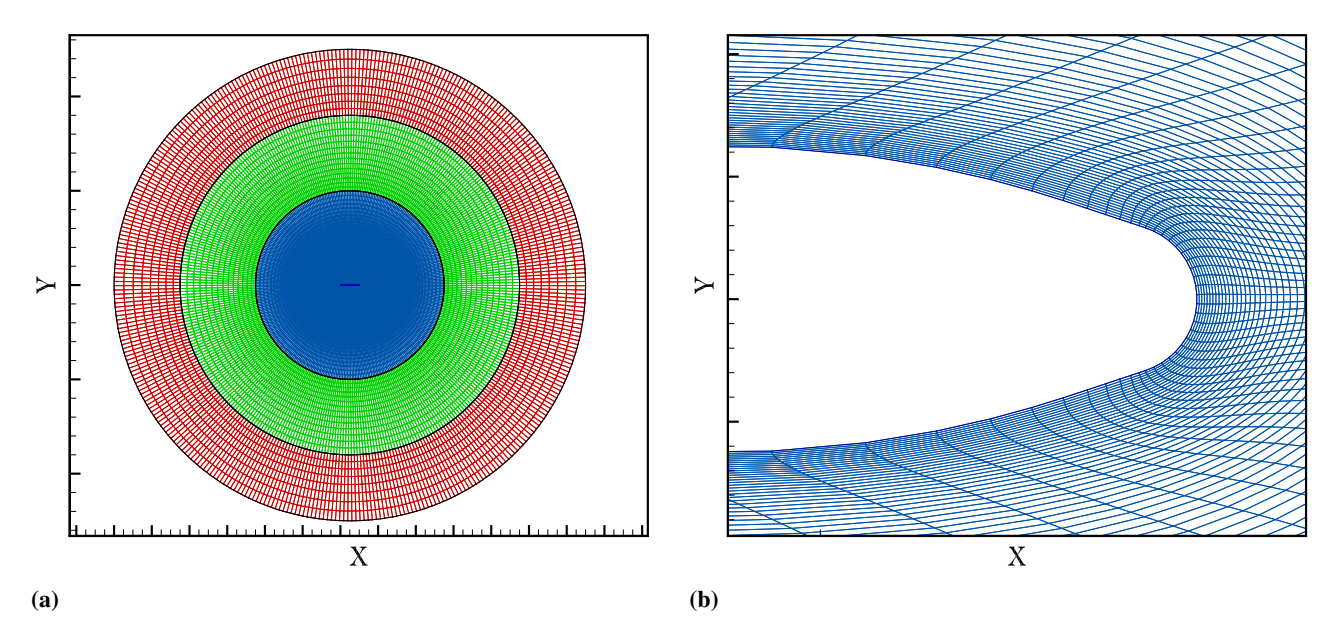


Fig. 3 The mesh around the flat plate. (a) The total mesh: the inner domain move sinusoidal, the intermediate mesh ring deforms dynamically and the outer mesh ring is fixed. (b) The mesh around leading and trailing edge of the plate (symmetric).

B. Solver Setup

Inviscid flow model is used for the simulations. The density based solver is considered for compressible flow with implicit formulation. Green-Gauss Node Based (GGNB) is selected for spatial gradient discretization and Second order upwind was chosen for the remaining spatial discretization. Second order implicit in transient formulation is chosen.

A pressure far-field is considered for the outer boundary. As the frequency of oscillation increase, the time period per cycle decrease. A number of 300 time steps per cycle is maintained for all computations ensuring that CFL < 1. The transient solution is initialized using converged steady state solution.

VI. Compressible Total Lift Frequency Response

The compressible total lift is computed for a plate performing a harmonically plunging motion. The theoretical results by Haskind [12] are validated against CFD results and compared to Theodorsen [3] incompressible lift at M=0. Figure 4 shows the total lift, L_{Tot} , normalized by the quasi-steady lift for three values of Mach number, M=0.35, 0.6 and 0.6. As shown in figure, the compressible lift shows a good agreement to the inviscid flow simulations even at high frequency values. It can be noticed that the lift magnitude decreases as Mach number increases. Moreover, at low frequency values, the compressible lift and phase shift are comparable to Theodorsen incompressible lift, showing that compressibility effect is small at low frequency values, however, the effect is significant at high frequencies.

VII. Conclusion

The aerodynamic loads of a plunging flat plate in a compressible fluid have a significantly different behaviour compared to the incomressible fluid. The total lift for the compressible fluid doesn't increase with frequency but converges to a steady constant value at high reduced frequency values. Moreover, the total lift magnitude decreases as the Mach number increases and the phase shift increases significantly for reduced frequency around 1, then decreases to zero asymptotically for high frequencies. Also, the fluid compressibility has a trivial effect on the aerodynamic loads at a low frequency, however, the effect is notable at high frequencies. The frequency response of the circulatory lift tends to decrease to a very small values as the frequency increase. The non-circulatory phase leads decreases as the frequency increase.

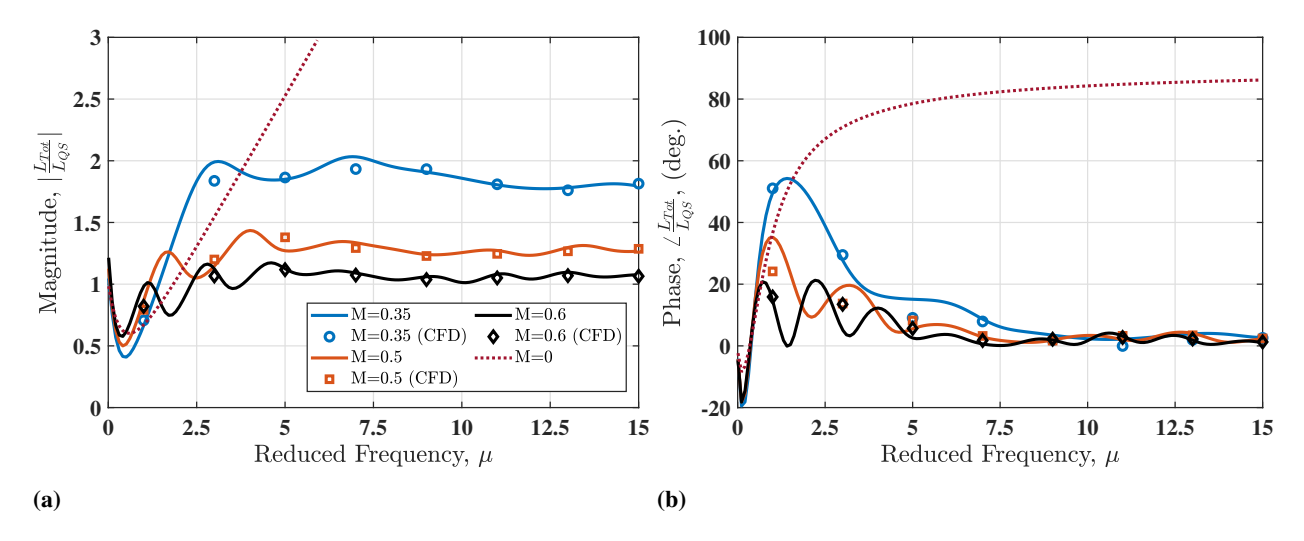


Fig. 4 Total lift frequency response comparison between analytical (solid lines), CFD results (markers) and incompressible potential flow, i.e Theodorsen's, (dotted line).(a) Total lift vs. reduced frequency. (b) Lift phase angle vs. reduced frequency.

Appendix

A. Angular and Radial Mathieu Functions

Mathieu functions are defined in the elliptic-cylinder coordinate system P.Moon [23]. As Mathieu functions have different notations we adopted notations given by Abramowitz [22]. As a reference for further reading, J.C. Gutierrez-Vega [24] summarized the most commonly used notations, for Mathieu functions. The angular Mathieu functions are classified into four categories as [22]

$$ce_{2r+p}(\zeta,q) = \sum_{k=0}^{\infty} A_{2k+p}^{2r+p} \cos(2k+p)\zeta \quad \text{where } (r \ge 0; \ p = 0,1), \tag{17}$$

$$se_{2r+p}(\zeta,q) = \sum_{k=0}^{\infty} B_{2k+p}^{2r+p} \sin(2k+p)\zeta \quad where \ (r \ge 0; \ p = 0,1),$$
 (18)

where A, B are expansion coefficients. The radial Mathieu equations of the fourth kind will be denoted as $Mc_{2r+p}^{(4)}$ and $Ms_{2r+p}^{(4)}$ where r=0,1,2,... and p=0,1. In our calculations, we used the expression given by [22]. The functions are defined as a product of Bessel functions and Hankel function of the second kind and have the form:

$$Mc_{2r}^{(4)}(\xi,q) = \frac{1}{\epsilon_s A_{2s}^{2r}} \sum_{k=0}^{\infty} (-1)^{k+r} A_{2k}^{2r}(q) \left[J_{k-s}(u_1) H_{k+s}^{(2)}(u_2) + J_{k+s}(u_1) H_{k-s}^{(2)}(u_2) \right]$$
(19)

$$Mc_{2r+1}^{(4)}(\xi,q) = \frac{1}{\epsilon_s A_{2s+1}^{2r+1}} \sum_{k=0}^{\infty} (-1)^{k+r} A_{2k+1}^{2r+1}(q) \left[J_{k-s}(u_1) H_{k+s+1}^{(2)}(u_2) + J_{k+s+1}(u_1) H_{k-s}^{(2)}(u_2) \right]$$
(20)

$$Ms_{2r}^{(4)}(\xi,q) = \frac{1}{B_{2s}^{2r}} \sum_{k=1}^{\infty} (-1)^{k+r} B_{2k}^{2r}(q) \left[J_{k-s}(u_1) H_{k+s}^{(2)}(u_2) - J_{k+s}(u_1) H_{k-s}^{(2)}(u_2) \right]$$
(21)

$$Ms_{2r+1}^{(4)}(\xi,q) = \frac{1}{B_{2s+1}^{2r+1}} \sum_{k=0}^{\infty} (-1)^{k+r} B_{2k+1}^{2r+1}(q) \left[J_{k-s}(u_1) H_{k+s+1}^{(2)}(u_2) - J_{k+s+1}(u_1) H_{k-s}^{(2)}(u_2) \right]$$
(22)

where $\epsilon_0 = 2$, $\epsilon_s = 1$, for $s = 1, 2, 3, ..., u_1 = \sqrt{q}e^{\xi}$, $u_2 = \sqrt{q}e^{-\xi}$ and A, B are the same expansion coefficients in Eqs.(17),(18). Mathieu functions are essential in the computation of the aerodynamic loads; therefore, validation of our MATLAB code, used in the function computations, is essential to provide in the results. Figure 5 shows a comparison between the results from MATLAB code and Abramowitz [22]. Figures 5a compares the even periodic

Mathieu functions for functions order from 1 to 3 at q = 1. The radial Mathieu function of first kind and zero order is shown in Fig. (5b) for four different values of q ranging from q = 0.75 to q = 3.75. For all q values, our calculations fall to an excellent agreement with Abramowitz.

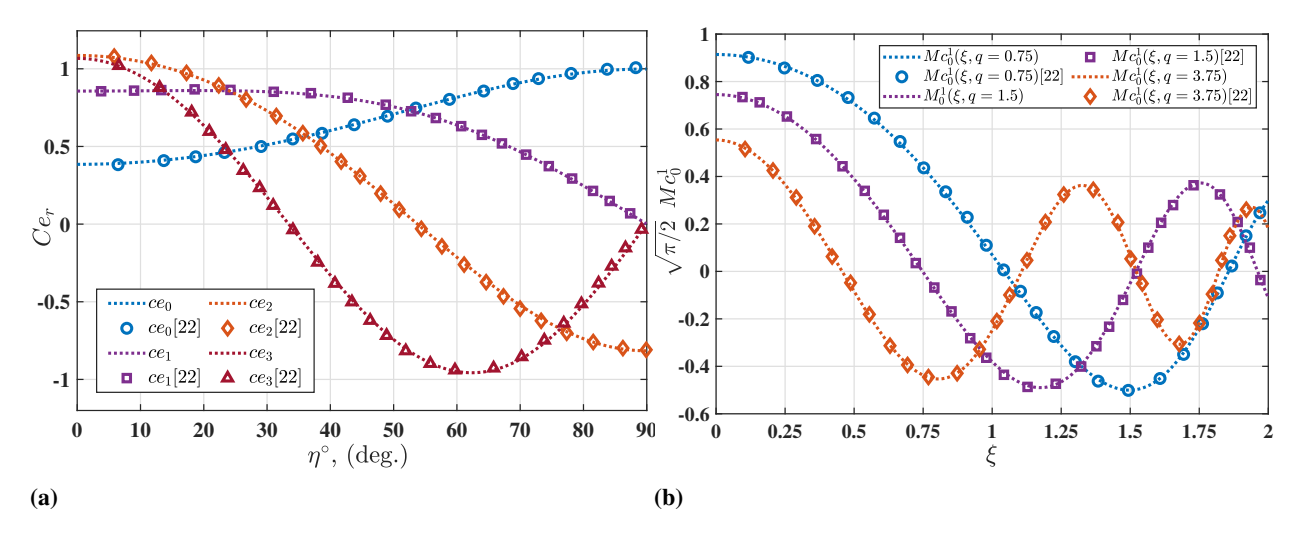


Fig. 5 Even periodic Mathieu functions.(a) Even periodic Mathieu functions at (q = 1) compared to Abramowitz [22].(b) Radial mathieu function of the first kind and zero order compared to Abramowitz.

As angular Mathieu functions are functions of elliptic angle ζ , q and eigenvector matrix N (see Apendix A). Bibby [25] recommended investigating the effect of the preceding variables on the accuracy of the summations as these parameters are application based. Double precision (15 decimal digits) is used in calculation using MATLAB Symbolic Math Toolbox and Variable Precision Arithmetic for high computational accuracy.

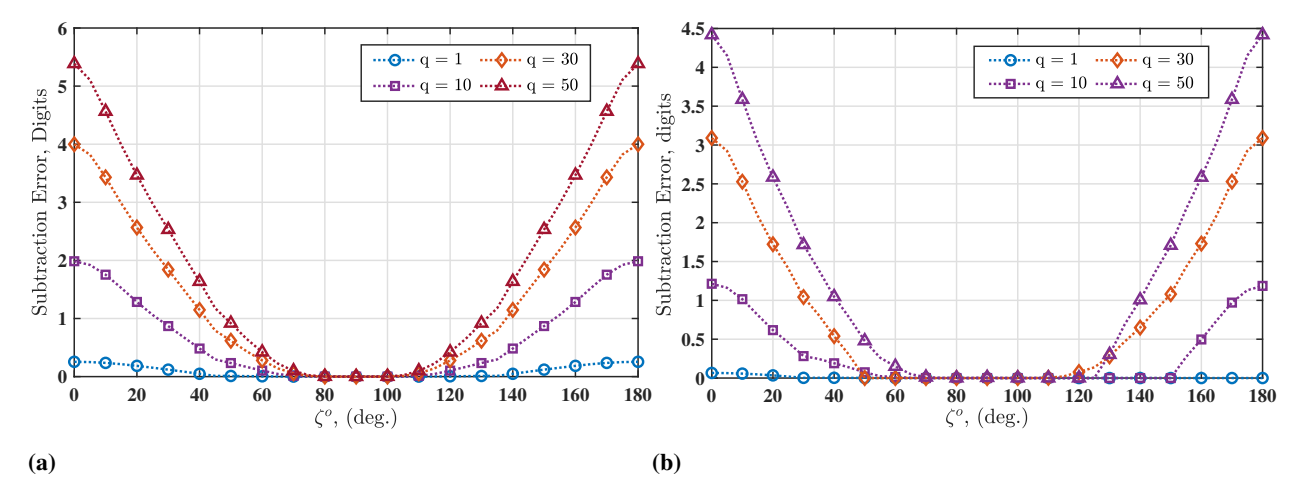


Fig. 6 Subtraction error versus the elliptic angle ζ at N=100. (a) Even angular Mathieu function of zero order $ee_0(\zeta,q)$. (b) Odd angular Mathieu function of first order $se_1(\zeta,q)$.

Figure (6a) shows the angle η effect on subtraction error [26] for the angular Mathieu function of zero order. As shown, the maximum error is associated with angle extremes $0, \pi$ with a value around 5 digits for q = 50, which exceeds our application range. Subtraction error for the odd Mathieu function of the first order is shown in Fig. (6b) with maximum errors at graph extreme locations for q = 50. From the previous discussion, it can be concluded that double precision computations are sufficient for accurate results.

B. Analytical solution on Infinite integral in Eqn. 15

For simplicity $\cos \zeta$ in Eqn. 15 will be replaced by x.

$$f(x) = e^{-i\nu x} \int_{\infty}^{1-x} e^{-i\nu\xi} H_0^{(2)}(\kappa\xi) d\xi$$
 (23)

expressing $H_o^{(2)}(z)$ as a linear combination of Bessel functions in the form $H_o^{(2)}(z) = J_o(z) - i Y_o(z)$ where

$$J_{o}(z) = \sum_{m=0}^{\infty} \frac{(-1)^{m} (z/2)^{2m}}{m! \Gamma(m+1)}$$

$$Y_{o}(z) = -\frac{1}{\pi} \sum_{m=0}^{n-1} \frac{(-m-1)!}{m!} \left(\frac{z^{2}}{4}\right)^{m} + \frac{2}{\pi} J_{o}(z) \ln(z/2) - \frac{2}{\pi} \sum_{m=0}^{\infty} \frac{\left(\frac{-z^{2}}{4}\right)}{m! m!} \psi(m+1)$$
(24)

The first summation of $Y_o(z)$ vanishes as the function order is zero (n = 0). Changing the variables of Eqn. 23 as follows

$$\kappa \xi = z, \quad d\xi = \frac{dz}{\kappa}, \quad , \xi = 1 - x \to z = \nu(1 - x), \quad \xi = \infty \to z = \infty$$
 (25)

Substituting Eqns. 24 and 25 into Eqn. 23 and labeling the resulting term as L_1, L_2 and L_3 , then

$$L_{1} = \int_{\kappa(1-x)}^{\infty} e^{-\frac{i\nu z}{\kappa}} \sum_{m=0}^{\infty} \frac{(-1)^{m} (z/2)^{2m}}{m! \Gamma(m+1)} = \sum_{m=0}^{\infty} \frac{(-1)^{m} (0.5)^{2m}}{m! \Gamma(m+1)} \int_{\kappa(1-x)}^{\infty} e^{-\frac{i\nu z}{\kappa}} z^{2m} dz$$

$$= \sum_{m=0}^{\infty} \frac{(-1)^{m} (0.5)^{2m} \Gamma(2m+1, \nu(1-x))}{m! \Gamma(m+1) (\frac{i\nu}{\kappa})^{(2m+1)}}$$
(26)

$$L_{2} = \frac{2}{\pi \kappa} \int_{\kappa(1-x)}^{\infty} e^{\left(\frac{-i\nu z}{\kappa}\right)} \sum_{m=0}^{\infty} \frac{(-1)^{m} (0.5)^{2m}}{m! \Gamma(m+1)} \ln\left(\frac{z}{2}\right) dz$$

$$= \frac{2}{\pi \kappa} \sum_{m=0}^{\infty} \frac{(-1)^{m} (0.5)^{2m}}{m! \Gamma(m+1)} \left[-\ln\left(2\right) \int_{\kappa(1-x)}^{\infty} e^{\frac{-i\nu}{\kappa} z} z^{2m} dz + \int_{\kappa(1-x)}^{\infty} e^{\frac{-i\nu}{\kappa} z} z^{2m} \ln\left(z\right) dz \right]$$
(27)

Applying appropriate change of variables and with the aid of Leibniz integral rule, the second integral of Eqn. 27 can be expressed as

$$\int_{\kappa(1-x)}^{\infty} e^{\frac{-i\nu}{\kappa}z} z^{2m} \ln(z) dz = \left(\frac{\kappa}{i\nu}\right)^{(2m+1)} \left[\frac{1}{2} \frac{d}{dm} \Gamma(2m+1, i\nu(1-x)) + \ln\left(\frac{\kappa}{i\nu}\right) \Gamma(2m+1, i\nu(1-x)) \right]$$
(28)

Substituting Eqn. 28 into Eqn. 27, L_2 have the form

$$L_{2} = \frac{2}{\pi \kappa} \sum_{m=0}^{\infty} \frac{(-1)^{m} (0.5)^{2m}}{m! \Gamma(m+1)} \times \left[-\ln(2) \left(\frac{i\nu}{\kappa} \right)^{(-2m-1)} + \left(\frac{\kappa}{i\nu} \right)^{(2m+1)} \left(\frac{1}{2} \frac{d}{dm} \Gamma(2m+1, i\nu(1-x)) + \ln\left(\frac{\kappa}{i\nu} \right) \Gamma(2m+1, i\nu(1-x)) \right) \right]$$
(29)

where

$$\frac{d}{dm} \Gamma(2m+1, i\nu(1-x)) = 2 \times \left[\Gamma(2m+1, i\nu(1-x)) \ln(i\nu(1-x)) + G_{23}^{30} \left({}_{0, 0, (2m+1)}^{1, 1} | i\nu(1-x) \right) \right]$$
(30)

$$L_{3} = \frac{2}{\pi} \sum_{m=0}^{\infty} \frac{\psi(m+1) (-0.25)^{m}}{(m!)^{2}} \int_{\kappa(1-x)}^{\infty} e^{\frac{-i\nu}{\kappa} z} z^{2m} dz = \frac{2}{\pi} \sum_{m=0}^{\infty} \frac{\psi(m+1) (-0.25)^{m} \Gamma(2m+1, \nu(1-x))}{(m!)^{2} (\nu/\kappa)^{(2m+1)}}$$
(31)

Finally, from Eqns. 23, 26, 29 and 31 the function f(x) can be expressed as

$$f(x) = e^{-i\nu x} \int_{\infty}^{1-x} e^{-i\nu\xi} H_0^{(2)}(\kappa\xi) d\xi = \frac{-1}{\kappa} e^{-i\nu x} \left[L_1 - i \left(L_2 - L_3 \right) \right]$$
 (32)

Acknowledgement

The authors would like to acknowledge the USAID for funding this research. The authors would like to thank Mahmoud Abdelgalil for the fruitful discussions on Mathieu functions. The authors would like to thank Dr Amir S. Rezaei,Ph.D. for his advice on implementing the CFD simulations. Finally, the first author would like to thank Carola Wright, Ph.D. for support and encouragement during implementing this research.

References

- [1] Lin, C., Reissner, E., and Tsien, H., "On two-dimensional non-steady motion of a slender body in a compressible fluid," *Journal of Mathematics and Physics*, Vol. 27, No. 1-4, 1948, pp. 220–231.
- [2] Miles, J. W., "Linearization of the Equations of Non-Steady Flow in a Compressible Fluid," *Journal of Mathematics and Physics*, Vol. 33, No. 1-4, 1954, pp. 135–143.
- [3] Theodorsen, T., and Mutchler, W., "General theory of aerodynamic instability and the mechanism of flutter," Tech. Rep. 496, NACA, 1935.
- [4] Taha, H. E., and Rezaei, A. S., "On the dynamics of unsteady lift and circulation and the circulatory-non-circulatory classification," *AIAA Scitech 2019 Forum*, 2019, p. 1853.
- [5] Possio, C., "L'azione aerodinamica sul profilo oscillante in un fluido compressibile a velocita iposonora," *L'aerotecnica*, Vol. 18, No. 4, 1938, pp. 441–458.
- [6] Schade, T., "Numerical Solution of the Possio Integral Equation of the Oscillating Aerofoil in a Two-Dtiensional Subsonic Flow. Part Iv-Numerical Part. Reps. and Translations No. 846," *British MAP V61kenrode*, 1947.
- [7] Dietze, "The Air Forces for the Harmonically Oscillating Aerofoil in a Compressible Medium at Subsonic Speeds: Two-dimensional Problem," ARC, Vol. 10, No. 219, 1946.
- [8] Miles, J. W., "A note on a solution of Possio's integral equation for an oscillating airfoil in subsonic flow," *Quarterly of Applied Mathematics*, Vol. 7, No. 2, 1949, pp. 213–216.
- [9] Jones, W., "Oscillating wings in compressible subsonic flow," Tech. Rep. R.M 2855, British Aeronautical Research Council, London, England, Oct. 1951.
- [10] Jones, W. P., "The oscillating aerofoil in subsonic flow," Tech. Rep. R.M 2921, Aeronautical Research Council, 1953.
- [11] Minhinnick, I., "Subsonic Aerodynamic Flutter Derivatives for Wings and Control Surfaces (Compressible and Incompressible Flow," Tech. Rep. 87, British R.A.E, 1950.
- [12] Haskind, M., "Oscillations of a Wing in a Subsonic Gas Flow." Russian Air Material Command and Brown Univ. Translation A9-T, Vol. 22, 1947, pp. 129–146.
- [13] Reissner, E., "On the application of Mathieu functions in the theory of subsonic compressible flow past oscillating airfoils," Tech. Rep. 2363, NACA, Washington, USA, May 1951.
- [14] Timman, R., "Beschouwingen over de luchtkrachten op trillende vliegtuigvleugels," Ph.D. thesis, Technische Hogeschool te Delft, Delft, Netherlands, 1946.
- [15] Timman, R., and Van de Vooren, A. I., Theory of the Oscillating Wing with Aerodynamically Balanced Control Surface in a Two-Dimensional, Subsonic, Compressible Flow, National Luchtvaartlaboratorium, 1949.
- [16] Mazelsky, B., "Theoretical aerodynamic properties of vanishing aspect ratio harmonically oscillating rigid airfoils in a compressible medium," *Journal of the Aeronautical Sciences*, Vol. 23, No. 7, 1956, pp. 639–652.
- [17] Hofsommer, D., "Systematic representation of aerodynamic coefficients of an oscillating aerofoil in two-dimensional incompressible flow," Tech. Rep. F 61, NLL, 1950.
- [18] Küssner, H., "A general method for solving problems of the unsteady lifting surface theory in the subsonic range," *Journal of the Aeronautical Sciences*, Vol. 21, No. 1, 1954, pp. 17–26.
- [19] Timman, R., Van de Vooren, A., and Greidanus, J., "Aerodynamic coefficients of an oscillating airfoil in two-dimensional subsonic flow," *Journal of the Aeronautical Sciences*, Vol. 18, No. 12, 1951, pp. 797–802.

- [20] Timman, R., Van de Vooren, A., and Greidanus, J., "Aerodynamic coefficients of an oscillating airfoil in two-dimensional subsonic flow," *Journal of the Aeronautical Sciences*, Vol. 18, No. 12, 1951, pp. 797–802.
- [21] Dietze, F., "Die Luftkräfte des harmonisch schwingenden Flügels im kompressiblen Medium bei Unterschallgeschwindigkeit," DVL Forschungsbericht 1733, 1943.
- [22] Abramowitz, M., and Stegun, I. A., *Handbook of mathematical functions with formulas, graphs, and mathematical tables*, Vol. 55, US Government printing office, 1948.
- [23] Moon, P., and Spencer, D. E., Field theory handbook: including coordinate systems, differential equations and their solutions, Springer, 2012.
- [24] Gutierrez-Vega, J. C., Rodriguez-Dagnino, R., Meneses-Nava, M., and Chavez-Cerda, S., "Mathieu functions, a visual approach," *American Journal of Physics*, Vol. 71, No. 3, 2003, pp. 233–242.
- [25] Bibby, M. M., and Peterson, A. F., "Accurate Computation of Mathieu Functions," *Synthesis Lectures on Computational Electromagnetics*, Vol. 8, No. 2, 2013, pp. 1–133.
- [26] Van Buren, A., and Boisvert, J., "Accurate calculation of the modified Mathieu functions of integer order." *Quarterly of applied mathematics*, Vol. 65, 2007, pp. 1–23.